Identification of Anomalous Muonium in Semiconductors as a Vacancy-Associated Center

N. Sahoo, K. C. Mishra, and T. P. Das
Department of Physics, State University of New York at Albany, Albany, New York 12222
(Received 30 March 1984; revised manuscript received 13 May 1985)

With use of a first-principles unrestricted Hartree-Fock cluster procedure, it is demonstrated that a (μ^+e^-) center trapped near a vacancy has all the features of the hyperfine tensors for anomalous muonium in diamond and silicon obtained from muon-spin-rotation measurements.

PACS numbers: 71.70.Jp, 71.55.Fr, 76.90.+d, 78.50.Ec

Measurements by the muon-spin-rotation technique[1] have revealed the existence of two muonium centers in semiconductors: normal muonium[2] (Mu), with isotropic hyperfine interaction which is a substantial fraction of that of free muonium, and anomalous muonium[2] (Mu*), with a weak and highly anisotropic hyperfine interaction. Recent theoretical investigations by a number of procedures[3-5] have supported a tetrahedral interstitial location for Mu. A number of models have been proposed[6,7] for Mu*, but no substantive investigations to test these models have yet been reported. On the other hand, muon-spin-rotation studies[2,8] have provided a wealth of experimental information regarding the hyperfine tensor (**A**) for Mu*. Thus, in elemental semiconductors, **A** has been found[2] to be oblate and axially symmetric about the $\langle 111\rangle$ axis, the components $|A_{\parallel}|$ and $|A_{\perp}|$ in megahertz being 167.9 and 392.5 in diamond, 16.8 and 92.6 in silicon, and 26.8 and 130.7 in germanium. The ratios $A_{\parallel}/A_{\perp}$ are found from the observed magnetic field dependence[2] of muon-spin-rotation frequencies to be negative for diamond and positive for silicon and germanium. Further, Mu to Mu* conversion studies[8] in diamond single crystals have indicated that $A_{\perp}$ is negative. In the present work, through a first-principles unrestricted Hartree-Fock investigation, it is demonstrated for the first time that (a) a (μ^+e^-) system can be trapped near a vacancy, and (b) the associated **A**, after vibrational averaging, has all the features observed in diamond and silicon, providing reasonable agreement with the experimental[2] $A_{\parallel}$ and $A_{\perp}$.

We have been led to this model through extensive investigations[9] on a number of other models proposed in the literature such as an excited muonium,[6] a muonium in the hexagonal interstitial region,[6] and a muonium at the center of the bond[7] between two host atoms. Our results for these models, which will be published separately, have shown that none of them can be considered as a viable one for Mu*, either from energy-minimum or predicted hyperfine-tensor considerations or both. However, these investigations have suggested that in the appropriate model, the unpaired spin orbital for Mu* should be comprised of host-atom orbitals directed toward the muon, a situation well represented in the vacancy-associated model used here. Support for this model for Mu* is also available from a recent measurement[10] of the blocking effect on channeling of positrons from muon decay, from infrared measurements,[11] which provide evidence for hydrogen trapping near vacancies, and from the near equality of measured[12] Mu* hyperfine tensors in GaP and GaAs. As we discuss later, the observed axial symmetry of **A** requires the (μ^+e^-) system to be trapped near a double positively charged vacancy (V^{+2}) site, or equivalently, the μ^+ to be trapped near a V^{+1} site, there being evidence for the latter from electron paramagentic resonance[13] measurements, while the stability of the V^{+2} center has been demonstrated theoretically.[14]

For our investigations, we have utilized the unrestricted Hartree-Fock LCAOMO (linear combination of atomic orbitals for molecular orbitals) procedure involving different spatial characters for orbitals of opposite sign, which had been successfully applied[3] earlier for Mu in diamond. In the case of Mu*, where **A** has axial symmetry, one needs both the Fermi contact and dipolar constants A and B which determine the components $A_{\parallel}=A+2B$ and $A_{\perp}=A-B$. The constants A and B in megahertz are given in the unrestricted Hartree-Fock (UHF) procedure by the relations

$$A=\tfrac{4}{3}\gamma_e\gamma_\mu\hbar(10^{-6}a_0^{-3})[\textstyle\sum_\nu\{|\psi_{\nu\uparrow}(\mathbf{R})|^2-|\psi_{\nu\downarrow}(\mathbf{R})|^2\}+|\psi_{u\uparrow}(\mathbf{R})|^2],$$
$$B=(\gamma_e\gamma_\mu\hbar/4\pi)(10^{-6}a_0^{-3})[\textstyle\sum_\nu\{\langle\psi_{\nu\uparrow}|O|\psi_{\nu\uparrow}\rangle-\langle\psi_{\nu\downarrow}|O|\psi_{\nu\downarrow}\rangle\}+\langle\psi_{u\uparrow}|O|\psi_{u\uparrow}\rangle], \quad (1)$$

with ν referring to the paired orbitals and u to the unpaired spin orbital. The position vector for the muon is given by **R**, and O is the dipole operator $(3\cos^2\theta-1/r^3)$, γ_e and γ_μ being the gyromagnetic ratios for the electron and the muon. The oblateness ($|A_{\parallel}|<|A_{\perp}|$) of **A** requires A and B to have opposite signs, making the spin-polarized nature of the UHF procedure important, since it has the ability to provide a negative sign for A.

An important question that one has to decide on is the choice of the charge and symmetry of the vacancy-associated environment of Mu*. Of the five charge states $V^{\pm 2}$, $V^{\pm 1}$, and V^0 known[13,14] for the vacancy in semiconductors, a $(\mu^+ e^-)$ system trapped near the $V^{\pm 2}$ and V^0 sites only can lead to the paramagnetic nature of the Mu* center. Of these three choices, as illustrated in Fig. 1, V^0 and V^{-2} can be ruled out from consideration of possible Jahn-Teller distortion, leading to a nonaxial **A** in contrast to the observed axial symmetry. Figure 1(a) presents the energy levels expected from the combination of the four sp^3 hybrid dangling bonds associated with V^0 before Jahn-Teller distortion occurs as a result of the presence of the partially filled threefold-degenerate T_2 level. Figure 1(b) presents the level structure when a $(\mu^+ e^-)$ system gets trapped near V^0. This center, which has C_{3v} symmetry, is Jahn-Teller unstable because of the partially filled twofold degenerate E level. After Jahn-Teller distortion [Fig. 1(c)], the axial symmetry is destroyed. An analogous situation occurs for the system $(\mu^+ e^-) + V^{-2}$ [Fig. 1(d)]. For the $(\mu^+ e^-) + V^{+2}$ shown in Fig. 1(e) and used in the present work, no Jahn-Teller effect is expected because the unpaired electron is in a nondegenerate A_1 state, appropriate for the observed axially symmetric **A** tensor.

The clusters of atoms used in our investigations can be described by Fig. 2. The first cluster used for both diamond ($C_4H_{12}Mu^*$) and silicon ($Si_4H_{12}Mu^*$) involves seventeen atoms composed of the host atoms B, C, D, and E surrounding the vacancy at A, each saturated with three hydrogen atoms and with the muon on the line EA at different positions on both sides of A. For study of convergence with respect to cluster size, two larger clusters also with threefold symmetry, namely $[C(Si)_{10}H_{18}Mu^*]$ and $[C(Si)_7H_{18}Mu^*]$ corresponding to 29 and 26 atoms (which in addition to host atoms B through E, include respectively I through N and F through H), have been used for muon positions above and below the vacancy, respectively, in both the semiconductors. The basis set we have used for our molecular orbitals corresponds to the STO−3G Gaussian functions[15] for the atomic orbitals of the carbon, silicon, muonium, and saturator hydrogens for the dangling bonds at cluster surfaces. This choice of basis set has been found to be satisfactory from earlier investigations[3] on normal muonium and surface-adsorbed atoms.[16]

The total energies of the seventeen-atom cluster for diamond and silicon obtained from our calculations is plotted as a function of the position of the muon on the ⟨111⟩ axis in Figs. 3(a) and 3(b). In both cases, there are two minima, one on each side of the vacancy A. The positions and natures of the minima were unchanged by use of the larger clusters described earlier, indicating that the smaller-cluster results are representative of the real solid-state system. The positions of the minima on the right in Figs. 3(a) and 3(b) are close to the C-H and Si-H bond distances from E, while those on the left are at about 70% of the distance from the vacancy A to the BCD plane. The fact that the first minimum is deeper for silicon than for diamond is perhaps a reflection of the greater strength of the Si-H bond as compared to C-H. For diamond, the larger depth of the minimum on the left as compared to the right indicates that the combined strength of the bonding between the muon and the three atoms B, C, and D is greater than the single bond with the atom E at the C-H bond distance. The two minima for both systems were found to be absolute ones since the energy increases on moving perpendicular to the ⟨111⟩ direction in the neighborhood of the minima. Thus, the trapping of the $(\mu^+ e^-)$ system near a V^{+2} site is well supported from energy considerations. The stabil-

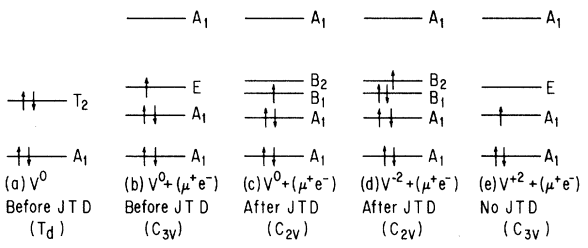

FIG. 1. Energy-level diagrams (schematic) for neutral vacancy V^0 and for $(\mu^+ e^-)$ trapped near V^0 and $V^{\pm 2}$. JTD represents Jahn-Teller distortion. The symmetries of the various centers are noted in the figure. The level orderings for $(\mu^+ e^-)$ located near V^0 and $V^{\pm 2}$ sites are obtained from cluster Hartree-Fock calculations.

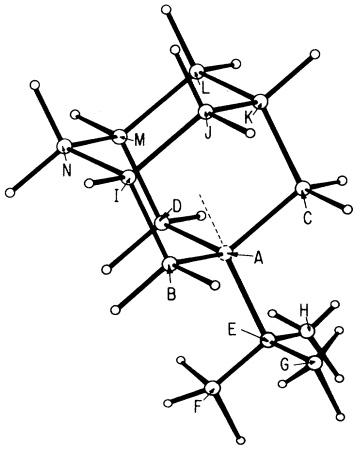

FIG. 2. Atomic environment associated with vacancy-associated model for Mu*. The vacancy is at A and the muon is located on the ⟨111⟩ axis shown by dotted lines.

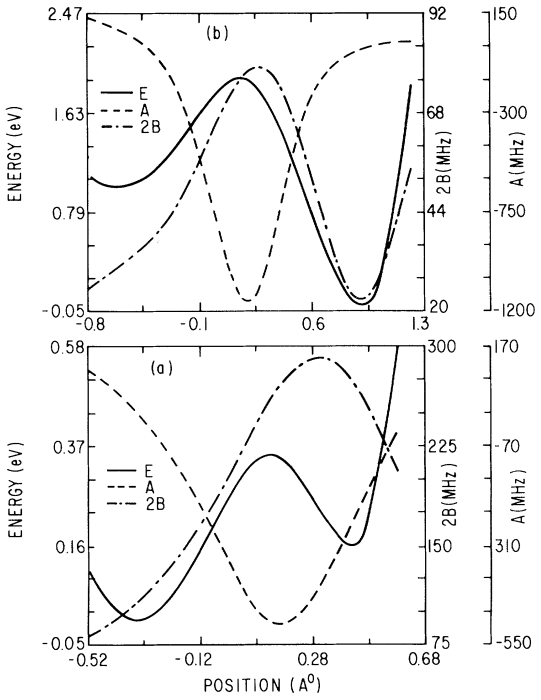

FIG. 3. Energy and hyperfine constants A and $2B$ for Mu* as a function of muon position along $\langle 111 \rangle$ axis (a) for diamond, (b) for silicon. The vacancy site is taken as the zero for the position of the muon, with the zeros of the potential energy curves being referred to the total energy at the deeper minimum in the two systems. On the left, all the curves are shown only up to the triangle BCD (Fig. 2).

ity of this vacancy-associated system could be considered as resulting from the extra attraction provided by the interaction of the positive charge of V^{+2} with the electron of the $(\mu^+ e^-)$ system. That this center corresponds to Mu* will now be demonstrated by analysis of the hyperfine properties using the calculated electronic wave functions and averaging them over the vibrational motions of the muon in the potentials represented by the energy curves in Figs. 3(a) and 3(b).

The contact and dipolar hyperfine constants A and $2B$ obtained with use of Eq. (1) are plotted as a function of muon positions in Figs. 3(a) and 3(b) for diamond and silicon. The contact term A is negative in most of the region covered in these figures, indicating the dominance of the exchange polarization contribution in Eq. (1) over the direct. The dipolar contribution is positive everywhere, the conditions for oblate **A** being thus satisfied over most of the region where the muon is trapped. The vibrational averaging of the hyperfine constants A and B has been carried out as in earlier work[3] on Mu. For this purpose, the vibrational wave functions appropriate for the potentials in Figs.

TABLE I. Experimental and theoretical values of $A_{\parallel}$ and $A_{\perp}$ in megahertz for Mu* in diamond and silicon.

Semiconductor	Experimental[a] $\lvert A_{\parallel} \rvert$	$\lvert A_{\perp} \rvert$	Sign[a] of $A_{\parallel}/A_{\perp}$	Theoretical $A_{\parallel}$	$A_{\perp}$
Diamond	167.9	392.5[b]	−	54	−155
Silicon	16.8	92.6	+	−23	−74

[a]Reference 2.
[b]The experimental sign of $A_{\perp}$ in diamond has been suggested to be negative (Ref. 8).

3(a) and 3(b) were obtained variationally with a basis set of twenty harmonic-oscillator eigenfunctions. For silicon, the vibrational wave function was totally localized in the deeper potential well on the right in Fig. 3(b), while in diamond it was mostly localized in the deeper well on the left, with only slight penetration into the region between the two wells. A one-dimensional averaging procedure is expected to be adequate here because of the rather slow variation found for A and B for muon motion perpendicular to the $\langle 111 \rangle$ axis.

After averaging[3] over the ground-vibrational wave function, the values for $\langle A \rangle$ and $\langle 2B \rangle$ were found to be −85 and 139 MHz for diamond leading to $A_{\parallel} = 54$ MHz and $A_{\perp} = -155$ MHz. For silicon, $\langle A \rangle = -55$ MHz and $\langle 2B \rangle = 32$ MHz, leading to $A_{\parallel} = -23$ MHz and $A_{\perp} = -71$ MHz. For purposes of ready comparison, the experimental values of $A_{\parallel}$ and $A_{\perp}$ in both diamond and silicon are listed in Table I along with our theoretical results. Our results provide agreement with all the observed features of the experimental data,[2] namely oblate **A** tensors with substantially larger components in diamond as compared to silicon, and positive sign for $A_{\parallel}/A_{\perp}$ in silicon and negative in diamond with $A_{\perp}$ negative.[8] The calculated values of $A_{\parallel}$ and $A_{\perp}$ also have the right order of magnitude as compared with experiment,[2] although somewhat underestimated in diamond. In attempting improvement in the magnitudes of the hyperfine constants, one would have to consider the influence of lattice distortions on the electronic energies and wave functions obtained by the UHF procedure as well as many-body effects. Both of these effects will involve formidable computational problems in view of the sizes of the clusters involved, but should be investigated in the future with advanced computing facilities.

However, the fact that the present model provides energetic evidence for trapping near the vacancy and explains all the features of the observed hyperfine tensors in diamond and silicon suggests that the vacancy-associated model may indeed be the proper one for

Mu^*. Additional evidences[10-12] of experimental nature supporting this conclusion have already been mentioned. It will be useful to study this model for germanium in the future, which is a somewhat more complicated task than in diamond and silicon because of the larger number of electrons involved. Finally, it is hoped that the availability of a viable model for Mu^* will be helpful in the understanding of the difficult questions of the mechanism for formation of Mu^* and its observed[2] stability at fairly high temperatures (>600 K) in diamond. As regards the first, the muon itself could produce the vacancy[17] at which it gets trapped to form the Mu^* center or might get trapped at an already existing vacancy site. The observation[18] of an increase in the strength of the Mu^* signal in electron-irradiated samples could be considered as supportive of the latter mechanism. The question of stability of the Mu^* center at fairly high temperatures is also an interesting one in view of the fact that monovacancies are considered to be mobile[19] at temperatures close to liquid nitrogen temperature. However, it is also known that centers corresponding to complexes of atoms with vacancies[19] are quite immobile with fairly high migration energies and annealing temperatures. One could thus expect the muonium-vacancy complex to be quite stable and immobile until reasonably high temperatures. This is of course a rather involved question and it is hoped that the success of the present model in explaining observed properties of anomalous muonium will stimulate further experimental and theoretical efforts to understand thoroughly all the factors that govern the stability and mobility of the Mu^* center as a function of temperature.

[1]J. H. Brewer, K. M. Crowe, F. N. Gygax, and A. Schenck, in *Muon Physics,* edited by V. W. Hughes and C. S. Wu (Academic, New York, 1975).

[2]E. Holzschuh *et al.*, Phys. Rev. A **25**, 1272 (1982), and references therein.

[3]N. Sahoo *et al.*, Phys. Rev. Lett. **50**, 913 (1983), and Hyperfine Interact. **17–19**, 525 (1984).

[4]M. Manninen and P. F. Meier, Phys. Rev. B **26**, 6690 (1982).

[5]H. Katayama-Yoshida and K. Shindo, Phys. Rev. Lett. **51**, 207 (1983).

[6]T. L. Estle, Hyperfine Interact. **8**, 365 (1978), and **17–19**, 585 (1984).

[7]M. C. R. Symons, Hyperfine Interact. **17–19**, 771 (1984).

[8]B. D. Patterson *et al.*, Hyperfine Interact. **17–19**, 605 (1984).

[9]Some of these models are briefly described in the second paper of Ref. 3. These and others will be described in detail in a separate publication.

[10]B. D. Patterson *et al.*, Phys. Rev. Lett. **52**, 938 (1984).

[11]H. J. Stein, Phys. Rev. Lett. **43**, 1030 (1979).

[12]R. F. Kiefl *et al.*, Bull. Am. Phys. Soc. **29**, 491 (1984).

[13]G. D. Watkins, in *Lattice Defects in Semiconductors, 1974,* edited by F. A. Huntley (Institute of Physics, London, 1975), p. 1.

[14]G. A. Baraff, E. O. Kane, and M. Schlüter, Phys. Rev. Lett. **43**, 956 (1979).

[15]W. J. Hehre, R. F. Stewart, and J. A. Pople, J. Chem. Phys. **51**, 2657 (1969).

[16]B. N. Dev *et al.*, Phys. Rev. B **29**, 1101 (1984).

[17]R. F. Kiefl *et al.*, Phys. Rev. B **32**, 530 (1985).

[18]E. Albert *et al.*, Hyperfine Interact. **15–16**, 525 (1983).

[19]M. Lanoo and J. Bourgoin, *Point Defects in Semiconductors I* (Springer-Verlag, New York, 1981), p. 229, and *Point Defects in Semiconductors II* (Springer-Verlag, New York, 1983), p. 269.